Advances in Modeling of Interconnect Materials

Blanka Magyari-Köpe[1] and Jeff Wu[2]
[1]Taiwan Semiconductor Manufacturing Company Technology Inc., San Jose, CA, USA, email: blankamk@tsmc.com
[2]Taiwan Semiconductor Manufacturing Company Ltd., Hsinchu, TW

2024 International Conference on Simulation of Semiconductor Processes and Devices (SISPAD) | 979-8-3315-1635-2/24/$31.00 ©2024 IEEE | DOI: 10.1109/SISPAD62626.2024.10733304

Abstract— Advanced systems scaling is encountering the so called "interconnect bottleneck", a challenge characterized by increased interconnect resistivities at reduced dimensions that affect signal transmission and lead to high power consumption. To overcome existing limitations and improve future chip performance, adoption of novel materials and processes will be critical. Atomistic material modeling is emerging as a crucial tool for broad spectrum material option evaluation and characterization, from simple metals to binary and ternary compounds, nanowires, and intercalated graphene. The paper reviews recent advancements and challenges in methodology development, addresses bulk, surface, grain boundary and contact effects and provides a discussion of their practical implementation for candidate materials.

I. INTRODUCTION

Integration of large number of transistors on a single chip requires complex interconnect solutions that can effectively manage signal propagation, power distribution, reliability, performance, and power consumption. Back-end-of-line (BEOL) Cu-based interconnects exhibit an exponential increase in resistance (R) at small dimensions. R coupled with the large parasitic capacitance (C) of the dielectric medium between metal lines, produces significant RC delays and impedes electron transport. To uphold BEOL performance, ensure precise signal transmission, reduce current-resistance drop and power consumption, *RC delay needs to be minimized.* Furthermore, to mitigate Cu's electromigration (EM) and dielectric breakdown issues, diffusion barrier and adhesion liner layers were integrated, which also impact resistivity and further reduce metal volume [1-2]. Consequently, there is increasing demand for *liner-free alternative materials with decreased EM tendencies, reduced barrier volumes, high thermal conductivity, and low resistivity* to supersede Cu in interconnect architectures.

In recent years, advanced material simulations for selection and optimization of potential interconnect materials have been systematically adopted [3-5] for evaluating and characterizing properties of a wide range of material options that encompass elemental metals, binary and ternary compounds, as well as nanowires and intercalated graphene. Furthermore, investigations have started focusing on low-k dielectric layer engineering [6-7] and electromigration tendency analysis. We are certainly witnessing a notable surge in enhanced precision model development for resistivity prediction that includes: 1) complex scattering mechanisms for interconnect structure design optimization; and 2) new material screening through quantum mechanical simulations for resistivity evaluation at reduced dimensions [8-13].

II. MECHANISMS AND SCATTERING MODELS

At small sizes, the rise in metal resistivity is primarily due to surface and grain-boundary (GB) scattering, which surpasses the contributions from the bulk material in scaled-down devices. Charge carrier transport in bulk metals can be determined from Boltzmann transport equation. Commonly used semiclassical Fuchs-Sondheimer (F-S) [14-15] and Mayadas-Shatzkes (MS) [16-17] models estimate resistivity due to surface and GB scattering to be proportional to $\rho_0 \times \lambda/d$, where λ - represents the intrinsic mean-free path of charge carriers, ρ_0 - is the bulk resistivity, and d - refers to film thickness for surface scattering or grain size for GB scattering. The F-S model employs Boltzmann transport formalism to describe electron relaxation in bulk, while accounts for diffuse surface scattering through boundary conditions. Specular scattering on smooth surfaces conserves momentum along direction of motion and attains a coefficient $p = 1$, while the momentum is lost in diffusive scattering regime and is described by $p = 0$ [18]. While the model is acceptable for thicker films, beyond $d < 20$ nm with increasing dominance of surface scattering, it presents severe shortcomings owing to its reliance on inadequate bulk-like model parameters.

As a key metric though, the $\rho_0 \times \lambda$ proxy has been widely used in material screening studies to establish resistivity trends. As poor conductivity leads to higher $\rho_0 \times \lambda$ values, the material search focused on identifying potential candidates with low ρ_0 or λ. Shorter λ than Cu (~40nm) induces reduced surface or GB scattering and may promote a particular material for potential solution even if its ρ_0 is higher than Cu. Within classical transport models $\rho_0 \times \lambda$ exhibits temperature independence and remains unaltered by impurity and defect electron scattering effects given that mechanisms increasing ρ_0 are proportionally decreasing λ and vice versa. Numerically obtainable from the Fermi surface, $\rho_0 \times \lambda$ does not require explicit electron-phonon interaction assessments or computationally intensive relaxation time ($\tau_n(k)$) calculations. To evaluate primary scattering mechanisms based on $\rho_0 \times \lambda$, two common approximations have been widely employed: 1) isotropic τ for phonon scattering dominated cases; 2) isotropic λ for regimes primarily influenced by impurity scattering.

***Grain boundary scattering*:** electron transport theory for several metals Cu, Co, Ru, Al, W, Pt, Rh, Ir, Ag, Au, Al, Ca, Ni, and Pd, was used to calculate electron transmission probabilities and/or conductances employing methods such as

ab initio complex band structure, non-equilibrium Green's function (NEGF) or Boltzmann transport [19-22]. The models suggest that reduced GB scattering is attainable if a material exhibits 1) larger grains than λ; or 2) low reflection coefficients; and prompt for improved growth process development to achieve desired material morphologies.

Surface scattering effects in thin metal layers primarily stem from surface potential perturbations caused by rough surfaces, misplaced atoms, or chemical contaminations. For very thin films, these perturbations can potentially lead to an increase in resistivity proportional to *1/d*, as predicted by an NEGF study that used frozen phonon approximation and one monolayer of surface roughness [23]. While electropositive metal surfaces were found to increase resistance by adatom charge transfer, electronegative metals minimize resistance through specular electron reflection [24]. These fundamental mechanisms underscore the importance of acquiring a deeper understanding of surface scattering effects and the pressing need to devise innovative engineering solutions through process control for its mitigation [25-26].

Resistivity anisotropy: Simulations and experimental studies pointed out anisotropic resistivity tendencies in W and Mo, with W (001) layers exhibiting higher resistivity than W (011) due to non-spherical Fermi surfaces and velocity distributions [27-28]. Anisotropy in resistivity originates from variations in electronic velocity components near surfaces due to morphology defined atomic level scattering mechanisms. Anisotropy effects are also prevalent in layered materials, where 2D conduction dominates. Generalizations of atomistic models to describe anisotropy through the conductivity tensor involved two considerations: 1) relaxation times determined by scattering mechanisms; and 2) group velocities near Fermi energy based on electronic band structure. The proposed solutions included: 1) $\rho_0 \times \lambda$ replacement by an R_{film}/R_{wire} proxy [29]; and 2) introduction of $\rho_0 \times \lambda$ transport tensor [12] inherently taking into account material symmetries; with both methods showing improved agreement with experiments.

Stability against EM: Cohesive energies and formation enthalpies have been assessed routinely as proxies for resistance against electromigration and to evaluate whether diffusion barrier layers are needed [30].

III. ELEMENTAL, BINARIES AND TERNARIES

Elemental metals have been the primary focus due to their superior conductivity. Co, Mo, W, Ru, and several Pt-group metals have gained attention given their desirable combined properties such as low bulk resistivity, short λ, high melting point, and excellent EM performance. Co and Ru exhibit low resistivity and excellent thermal stability. In the limit of 6 nm lines, Ir, Rh and Ru stand out as competitive options given their $\rho_0 \times \lambda$, however GB resistivities still favor Cu [3].

Binary intermetallic compounds: 1000 alloys were recently surveyed based on combinations of Al, Cu, Ru, Mo, and Zn [30]. NiAl, Al_3Sc, and Cu-rich $Cu_{1-x}Al_x$ stand for low-resistivity options relative to disordered systems in which charge carrier scattering further increases resistivity. Current challenges involve controlling film stoichiometry, phase separation and interfacial composition, all critical properties for electromigration engineering [31]. $CuAl_2$, while exhibits a resistivity size effect similar to W and Co, its interface engineering with SiO_2 with an effective Al oxide diffusion barrier potential makes it attractive as a liner material [32]. Similarly, CuTi gains enhanced stability from a thin Ti oxide interface layer formation with SiO_2 [33]. Al_3Sc, on the other hand, shows promise due to its λ = 7 nm [34] but suffers from secondary phase formation and surface oxidation.

***Semimetals and topological materials*:** Topological metals, such as CoSi have conduction dominated by Fermi-arc surface states that suppress scattering [35,36], however exhibit higher bulk resistivities than Cu. NbAs Weyl metal can attain potentially 10*x* drop in resistivity from bulk to 200 nm [5,37].

Ternary $M_{n+1}AX_n$ (MAX)* ceramics compounds** are known for their high melting points, excellent thermal and electrical conductivity, and strong resistance to oxidation. Consisting of an early transition metal ***(M), an element from columns 13 or 14 ***(A)***, and carbon or nitrogen ***(X)***, they can be stabilized in various stoichiometries that include single phase 211, or 312 and 413 presenting α and β polymorphs. Extensive first-principles screening studies based on $\rho_0 \times \lambda$ for 170 crystal structures [38] yielded several potential carbon-based candidates with V, Ti or Ta for ***M*** and Al, Si, Ga, Ge, In, Cd or Sn for ***A*** with promising resistivity and scalability compared to Ru [38,39]. Nitrogen based phases demonstrate low $\rho_0 \times \lambda$ at the cost of reduced stability, however, represent still potential options over Cu. Although the anisotropic MAX 2D conduction is ideal for thin films, limitations are faced for wires. Furthermore, integration challenges relating to grain orientation control and (001) texture engineering during material deposition will need to be solved.

IV. INTERCALATED GRAPHENE

The quest for advanced resistivity scaling into low dimensions extended materials research into 2D materials, such as graphene. Intercalation of P-type materials such as SbF_5, $FeCl_3$, $SbCl_5$, $MoCl_5$, and $NbCl_3$ enhances graphene's electrical performance by facilitating charge transfer and Fermi level modulation that boost carrier concentrations [40-45]. FeCl3, selected for its low toxicity, can induce 9.9 Å increase in interlayer spacing and 0.64 eV shift in Fermi level, that yields below 5 μΩ·cm resistivities in films under 150 Å surpassing Cu (Fig. 1 a, b). Yet, meeting advanced node specifications will require further optimization and contact metal engineering solutions.

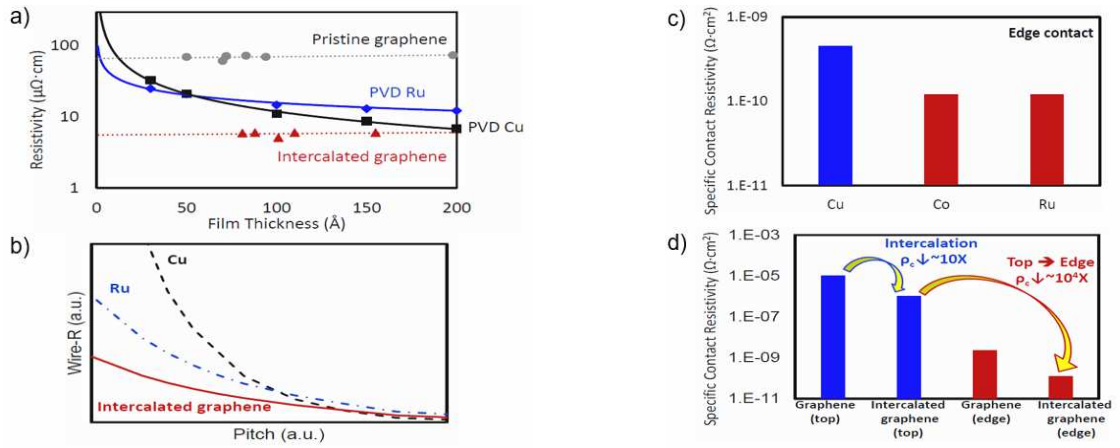

Fig. 1. Scaling properties of intercalated graphene with a) film thickness and b) metal pitch.
c) Contact metal screening for specific contact resistivity. d) Contact resistance improvement of P-type intercalated graphene with edge contact.

Contact resistance between intercalated graphene and metal

Graphene's adoption has been hindered by inherently high contact resistances induced by its semimetal properties and van der Waals gap that impedes the formation of Ohmic contacts with metals. Co and Ru contacts were predicted by NEGF simulations to achieve lowest specific contact resistivity (ρ_c), and experiments for oxidation resistant Ru confirmed the simulation trend [44]. Furthermore, models and experiments both indicated that $FeCl_3$ intercalated graphene benefits from edge contact geometry that presents significantly lower ρ_c (Fig. 1 c, d).

Material screening for contact resistance reduction

To explore alternative intercalants, an effectively constructed simulation framework examined the effects of varying concentrations of optimally distributed molecular and metallic intercalants into graphene bilayer interstitial regions. The model accounted for phonon contributions through thermally induced structural perturbations and statistical ensemble averages [46,47]. The calculated ρ_c values were mapped onto two physical descriptors: 1) equilibrium interlayer distance (d_{eq}); and 2) Fermi level shift from Dirac cone (E_D). Regression analysis across ranges of (4.5-9.37 Å) for d_{eq} and (-2, 2 eV) for E_D for both P- and N-type intercalants yielded linear ρ_c dependence on d_{eq} and $1/\sqrt{E_D}$. At 300 K, N-type intercalants induce significantly lower ρ_c over P-type options (Fig. 2 a, b), making them attractive options for experimental exploration of tailored material deposition and intercalation processes capable to address high boiling points.

V. SUMMARY AND OUTLOOK

Advanced material simulations have achieved substantial progress over the past few years in aiding interconnect material development as illustrated by the vast range of

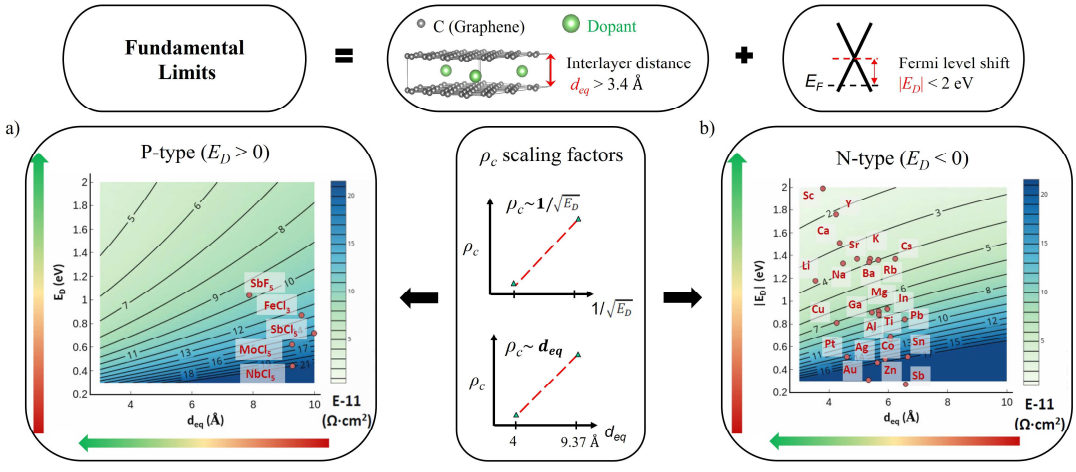

Fig. 2. Contact resistivity screening of a) P and b) N-type dopant intercalation into graphene.

material systems characterized. Highlights that further define scientific directions for aiding the quest of novel interconnect development include: 1) atomistic characterization of interconnect-dielectric interface with accurate description of scattering and thermal conductivity; and 2) efficient simulation algorithms for intricate interconnect structures.

ACKNOWLEDGEMENTS

The authors acknowledge C.H. Hsu and the experimental team S.W. Li, Y.C. Chan, S.Y. Yang, K.Y. Liao, C.H. Ho, C.Y. Chen, H.P. Chen, M.H. Lee, and W. Shu for in-depth discussions and for providing measured data.

REFERENCES

[1] L. Chen et al., "Interdiffusion Reliability and Resistivity Scaling of Intermetallic Compounds as Advanced Interconnect Materials", *J. Appl. Phys.* 129, 2021.
[2] K. Barmak et al., "Epitaxial Metals for Interconnects Beyond Cu", *J. Vac. Sci. Technol. A* 38, 033406, 2020.
[3] D. Gall et al., " Narrow Interconnects: The Most Conductive Metals", *IEEE International Electron Devices Meeting*, 2020.
[4] J. H. Moon et al., "Materials Quest for Advanced Interconnect Metallization in Integrated Circuits", *Adv. Sci.* 10, 2207321, 2023.
[5] D. Gall et al., "Materials for Interconnects," *MRS Bulletin* 1, 2021.
[6] C.M. Lin et al., "Ultralow-k Amorphous Boron Nitride Based on Hexagonal Ring Stacking Framework for 300 mm Silicon Technology Platform", *Adv. Mat. Techn.* 7, 2200022, 2022.
[7] B. Magyari-Köpe et al., "Quantum Mechanical Modeling Techniques for High-Performance Low-k Amorphous Material Engineering: a Showcase for aBN", *International Conference on Simulation of Semiconductor Processes and Devices*, 2023.
[8] D. Gall, "The Search for The Most Conductive Metal for Narrow Interconnect Lines", *J. Appl. Phys.* 127, 2020.
[9] A. Ramdas et al., "A Multi-Objective Approach for Rapid Identification of Post-Cu Interconnect Candidates", *International Symposium on VLSI Technology, Systems and Applications*, 2022.
[10] K. Zhao et al., "Mechanisms of Scaling Effect for Emerging Nanoscale Interconnect Materials", *Nanomaterials* 12, 1760, 2022.
[11] B. Van Troeye et al., "First-Principles Investigation of Thickness-Dependent Electrical Resistivity for Low-Dimensional Interconnects", *Phys. Rev. B* 108, 125117, 2023.
[12] K. Moors et al., "First-Principles-Based Screening Method for Resistivity Scaling of Anisotropic Metals", *Phys. Rev. Mat.* 6, 123804, 2022.
[13] C. Adelmann et al., "Alternative Metals: From *Ab Initio* Screening to Calibrated Narrow Line Models", *IEEE International Interconnect Technology Conference*, 154, 2018.
[14] K. Fuchs, "The Conductivity of Thin Metallic Films According to The Electron Theory of Metals", *Math. Proc. Cambridge Philos. Soc.* 34, 100, 1938.
[15] E. H. Sondheimer, "The Mean Free Path of Electrons in Metals", *Adv. Phys.* 1, 1, 1952.
[16] A. F. Mayadas and M. Shatzkes, "Electrical-Resistivity Model for Polycrystalline Films: The Case of Arbitrary Reflection at External Surfaces", *Phys. Rev. B* 1, 1382, 1970.
[17] A. F. Mayadas et al., "Electrical Resistivity Model for Polycrystalline Films: The Case of Specular Reflection at External Surfaces", *Appl. Phys. Lett.* 14, 345, 1969.
[18] M.-S. Kim et al., "Scaling Properties of Ru, Rh, and Ir for Future Generation Metallization", *J. Electron Device Society* 11, 399, 2023.
[19] A. Jog and D. Gall, "Electron Scattering at Surfaces and Grain Boundaries in Rh Layers", *IEEE Trans. Electron Dev.* 69, 3854, 2022.
[20] T. Zhou et al., "First-Principles Prediction of Electron Grain Boundary Scattering in fcc Metals", *Appl. Phys. Lett.* 120, 2022.
[21] S.J. Aboud et al., "*Ab Initio* for Design-Technology Co-Optimization", *Proc. SPIE* 11614, 2021.
[22] T. Markussen et al., "Grain Boundary Scattering in Ru and Cu Interconnects", *IEEE International Interconnect Technology Conference*, 2020.
[23] T. Zhou and D. Gall, "Resistivity Scaling due to Electron Surface Scattering in Thin Metal Layers", *Phys. Rev. B* 97, 165406, 2018.
[24] A. Jog et al., "Effect of Electronegativity on Electron Surface Scattering in Thin Metal Layers", *Appl. Phys. Lett.* 120, 2022.
[25] S.S. Ezzat et al., "Resistivity and Surface Scattering of (0001) Single Crystal Ruthenium Thin Films", *J. Vac. Sci. & Techn. A* 37, 2019.
[26] E. Milosevic and D. Gall, "Copper Interconnects: Surface State Engineering to Facilitate Specular Electron Scattering", *IEEE Trans. Electron Dev.* 66, 2692, 2019.
[27] Jog et al., "Anisotropic Resistivity Size Effect in Epitaxial Mo (001) and Mo (011) Layers", *Nanomaterials* 13, 957, 2023.
[28] P. Zheng and D. Gall, "The Anisotropic Size Effect of the Electrical Resistivity of Metal Thin Films: Tungsten", *J. Appl. Phys.* 122, 135301, 2017.
[29] S. Kumar et al., "Ultralow Electron-Surface Scattering in Nanoscale Metals Leveraging Fermi-Surface Anisotropy", *Phys. Rev. Mat.* 6, 085002, 2022.
[30] C. Adelmann *et al.,* "Intermetallic Compounds as Alternatives to Copper for Advanced Interconnect Metallization", *IEEE International Interconnect Technology Conference*, 2023.
[31] J.P. Soulié et al., "CuAl Films as Alternatives to Copper for Advanced Interconnect Metallization", *arxiv:2405.02046*, 2024.
[32] M. Zhang and D. Gall, "Resistivity Scaling in Epitaxial $CuAl_2$ (001) Layers", *IEEE Trans. Electron Dev* 69, 5110, 2022.
[33] M. Zhang and D. Gall, "CuTi as Potential Liner-And Barrier-Free Interconnect Conductor", *IEEE Trans. Electron Dev.* 71, 3252, 2024.
[34] J.P. Soulié et al., "Al_3Sc Thin Films for Advanced Interconnect Applications", *Microelectronic Engineering* 286, 112141, 2024.
[35] C.-T. Chen et al., "Topological Semimetals for Scaled Back-End-Of-Line Interconnect Beyond Cu", *IEEE International Electron Devices Meeting*, 2020.
[36] S.-W. Lien et al., "Unconventional Resistivity Scaling in Topological Semimetal CoSi", *Nature Quantum Materials* 3, 2023.
[37] S. Kumar et al., "Surface-Dominated Conductance Scaling in Weyl Semimetal NbAs", *Nature Comput. Materials.* 10, 84, 2024.
[38] K. Sankaran et al., "*Ab Initio* Screening of Metallic MAX Ceramics for Advanced Interconnect Applications", *Phys. Rev. Mat.* 5, 056002, 2021.
[39] M. Zhang et al., "Resistivity Scaling in Epitaxial Max-Phase Ti4SiC3 (0001) Layers", *J. Appl. Phys.* 130, 2021.
[40] A. Naeemi and J. D. Meindl, "Conductance Modeling for Graphene Nanoribbon (GNR) Interconnects", *IEEE Electron Dev. Lett.* 28, 428, 2007.
[41] D. Zhan et al., "$FeCl_3$ Based Few-Layer Graphene Intercalation Compounds: Single Linear Dispersion Electronic Band Structure and Strong Charge Transfer Doping", *Adv. Funct. Mater.* 30, 2003504, 2020.
[42] T. Misawa et al., "Line Width Dependence of Transport Properties in Graphene Nanoribbon Interconnects with Real Space Edge Roughness Determined by Monte Carlo Method", *Jpn. J. Appl. Phys.*, Vol. 54, P. 05eb01, 2015.
[43] Y. Yin et al., "Graphene, A Material for High Temperature Devices – Intrinsic Carrier Density, Carrier Drift Velocity and Lattice Energy", *Sci Rep* 4, 5758, 2014.
[44] S.W. Li et al., "Intercalated Graphene As Next Generation Back-End-Of-Line Conductors", *IEEE International Electron Devices Meeting,* 2023.
[45] J. Jiang et al., "Intercalation Doped Multilayer-Graphene-Nanoribbons for Next-Generation Interconnects", *Nano Lett.* 17, 1482, 2017.
[46] T. Markussen et al., "Electron-Phonon Scattering from Green's Function Transport Combined with Molecular Dynamics: Applications to Mobility Predictions", *Phys. Rev. B* 95, 245210, 2017.
[47] S. Smidstrup et al., "QuantumATK: An Integrated Platform of Electronic and Atomic-Scale Modelling Tools", *J. Phys. Cond. Matter* 32, 015901, 2020.